



HAL
open science

Optimization of an ultrafast OASLM using photoexcitations in organic thin films: the incoherent-to-coherent conversion efficiency of spectral concentration

Jean-Michel Nunzi, Fabrice Charra, Nicola Pfeffer

► **To cite this version:**

Jean-Michel Nunzi, Fabrice Charra, Nicola Pfeffer. Optimization of an ultrafast OASLM using photoexcitations in organic thin films: the incoherent-to-coherent conversion efficiency of spectral concentration. *Journal de Physique III*, 1993, 3 (7), pp.1401-1411. 10.1051/jp3:1993208 . jpa-00249007

HAL Id: jpa-00249007

<https://hal.science/jpa-00249007>

Submitted on 4 Feb 2008

HAL is a multi-disciplinary open access archive for the deposit and dissemination of scientific research documents, whether they are published or not. The documents may come from teaching and research institutions in France or abroad, or from public or private research centers.

L'archive ouverte pluridisciplinaire **HAL**, est destinée au dépôt et à la diffusion de documents scientifiques de niveau recherche, publiés ou non, émanant des établissements d'enseignement et de recherche français ou étrangers, des laboratoires publics ou privés.

Classification

Physics Abstracts

42.30 — 42.65 — 42.70F — 42.80K

Optimization of an ultrafast OASLM using photoexcitations in organic thin films : the incoherent-to-coherent conversion efficiency of spectral concentration

Jean-Michel Nunzi, Fabrice Charra and Nicola Pfeffer

Commissariat à l'Énergie Atomique, Direction des Technologies Avancées, Léti, Département d'Électronique et d'Instrumentation Nucléaire, Service de Physique Electronique, Saclay, 91191 Gif-sur-Yvette, France

(Received 10 December 1992, accepted 4 May 1993)

Résumé. — Les modulateurs spatiaux de lumière à adressage optique sont caractérisés en termes de densité d'éléments de résolution (pixel), de sensibilité à l'exposition et de temps de commutation. Les matériaux optiques non linéaires du troisième ordre sont attrayants afin d'améliorer les performances en termes de densité d'éléments de résolution et de vitesse de commutation. Ils sont comparés à l'aide de figures de mérite appropriées. Le photochromisme picoseconde de certains oligomères conjugués en fait les matériaux prototypes d'un convertisseur incohérent à cohérent ultra-rapide en film mince. La concentration spectrale est la caractéristique clef permettant d'atteindre de grandes sensibilités à l'exposition au niveau moléculaire. Des règles d'ingénierie moléculaire de la concentration spectrale sont proposées. Les oligomères conjugués de polycycles linéaires ont la structure qui convient à l'obtention d'une sensibilité d'exposition de 1 pJ/pixel dans le domaine des fréquences allant du MHz au GHz.

Abstract. — Optically addressed spatial light modulators are characterized in terms of pixel density, exposure sensitivity and switching time. Third order nonlinear optical materials are attractive in order to improve on pixel density and switching speed. They are compared using appropriate figures of merit. The picosecond photochromism of some conjugated oligomers makes them prototype materials for thin film incoherent to coherent optical converters. Spectral concentration is identified as the key feature which permits spectrally large exposure sensitivities in single molecules. Molecular engineering rules of the spectral concentration are proposed. Conjugated oligomers of linear polycycles have the required structure in order to achieve 1 pJ/pixel exposure sensitivity in the MHz to GHz frequency range.

Introduction.

In the field of image and beam processing, there is great need for devices in which a light-intensity profile can be recorded and transformed into a transmission or a phase retardation profile. This is the role of optically addressed spatial light modulators (OASLM) [1]. A special

class of such devices is the incoherent to coherent optical converter (ICOC) which permits the achievement of input functions in optical image processors based on holographic and Fourier optics. The most trivial representative of this class is the silver-halide photographic recording plate [2]. Usually, a real image is recorded under incoherent illumination on a photographic film, the developed slide then modulates a coherent beam for optical processing of the image. The drawback of silver-halide photography is the delay, close to one minute, between exposure and processing. Different techniques permit the realization of real time incoherent to coherent optical converters. In this paper, we first discuss some material requirements aimed at optimizing an ICOC with the possibilities offered by third-order nonlinear optical ($\chi^{(3)}$) materials. We then report on a new feature of the photochromism of organic molecules, *spectral concentration*, which is exhibited by a class of conjugated oligomers: α -oligothiophenes. Spectral concentration appears as the key feature for improved incoherent to coherent conversion efficiency. Physico-chemical analysis of the process is used to define molecular engineering rules which are at the origin of spectral concentration and which permit its practical use. We conclude with prospects towards using organic thin films for ultrafast incoherent to coherent optical conversion purposes.

Materials requirements.

As in photographic techniques, two functions characterize OASLMs: the exposure or recording and the readout. In usual (commercial) real time OASLMs, recording is performed using a photoconductor in order to optically switch the voltage applied across an electro-optic material which then modulates the readout beam [1]. This is the case in photoconductor — liquid-crystal light valves [3, 4]. In photorefractive and in self electro-optic devices [5, 6], both functions are performed in the same material. Basically, OASLMs may be characterized by their spatial resolution (Ab in cycle/mm), exposure sensitivity per pixel (W in pJ/px) where the pixel is defined as the smallest resolution element, and switching time (τ in s). Typical properties of OASLMs are displayed in table I.

In order to exploit the parallel addressing capabilities of light, an optimized OASLM should have a spatial resolution limited by diffraction ($Ab \approx \lambda^{-1} \approx 10^3$ cycle/mm). This determines the maximum thickness of the device. Consider the waist of a Gaussian beam at the focal point

Table I. — *Typical performances of OASLMs.*

| OASLM | Ab (cycle/mm) | W (pJ/px) | τ (s) | Ref. |
|-------------------------|-----------------|-------------|------------------------|------|
| Nematic liquid crystal | 60 | 5 | 0.01 | 3 |
| Ferro. liquid crystal | 100 | 0.2 | 10^{-4} | 4 |
| Photorefractive crystal | 300 | 100 | 0.1 | 5 |
| Self Electro-Optic | 12 | 180 | 10^{-6} | 6 |
| Quantum well etalons | 100 | 100 | 10^{-8} | 7 |
| Silver halide films | 10^3 | 10^{-2} | 100 | 2 |
| Prospective | 10^3 | 1 | 10^{-6} - 10^{-10} | |

of a lens, its radius w is connected to the Rayleigh range z_0 by $z_0 = \pi w^2/\lambda$, λ being the wavelength. Resolution is thus maximum (Tab. I) when device thickness is $t \leq \lambda$.

The speed of charge-transfer OASLMs is limited by carrier drift and capacitance [3-6]. In order to achieve high speed performances in the 10^6 to 10^{10} Hz range (Tab. I), a recognized route is the use of materials with large third-order nonlinear optical properties such as quantum confined semiconductor heterostructures [7] or organic semiconducting polymers [8]. Those materials are characterized by a susceptibility $\chi^{(3)}$ describing the complex index change $\delta n = 2 n_2 I$ induced on a read beam by a write (pump) beam of intensity I :

$$\delta n = 3 \chi^{(3)} I / 2 \varepsilon_0 c n^2. \quad (1)$$

The complex phase retardation variation induced inside the material is

$$\delta \varphi = \delta \varphi' + i \delta \varphi'' = 2 \pi (\delta n' + i \delta n'') t / \lambda. \quad (2)$$

In order to achieve a contrast ratio of 10 for the device transmission $T = \exp(-2 \delta \varphi'')$, the imaginary part of the phase retardation must reach $\delta \varphi'' \approx 1.2$. The same $\delta \varphi'$ value is large enough to reach the limiting 34 % diffraction efficiency $\eta \approx |\delta \varphi / 2|^2$ of thin phase holographic gratings [9]. As $t \approx \lambda$, the required index change necessary for efficient modulation is $\delta n \approx 0.2$.

For $\chi^{(3)}$ materials to be efficient OASLMs, the write process also needs to be optimized. In view of table I, a realistic switching energy is $W \approx 1$ pJ/px. With pixels of $1 \mu\text{m}^2$, this corresponds to an average energy consumption $I \tau \approx 100 \mu\text{J}/\text{cm}^2$. Using equation (1), this sizes the magnitude of materials optical nonlinearity to work as active elements in thin film OASLMs:

$$\chi^{(3)} / \tau = 2 \varepsilon_0 n^2 c \delta n / 3 I \tau \geq 10^{-3} \text{ m}^2 \text{ V}^{-2} \text{ s}^{-1}. \quad (3)$$

The nonlinearity is also alternatively expressed in terms of nonlinear index n_2 [10]. Its useful range is $n_2 / \tau \geq 0.1 \text{ m}^2/\text{J}$. For a 1 ns switching time, we need $\chi^{(3)} \geq 10^{-4} \text{ esu}$ ($1 \text{ m}^2 \text{ V}^{-2} = 7.2 \times 10^7 \text{ esu}$). Such a magnitude is achieved only when optical-field frequencies are close to resonance with real transitions.

In order to evaluate the optical modulation potentialities of nonlinear materials, we must estimate the magnitude of resonant nonlinearities in terms of elementary material parameters. We consider an assembly of non-interacting molecules described by a quantum three-level system. Molecules in the ground state g are excited in resonance using a recording beam at frequency ω_e . The excited state e has a lifetime τ . The induced absorption from the excited state e to the final state f is tested in resonance using a readout beam at frequency ω_r . For a homogeneous isotropic assembly of one-dimensional (rod-shaped) molecules with density N , the resonant part of the relevant third-order nonlinear optical susceptibility can be written:

$$\chi^{(3)} = \text{Im} (\chi^{(1)}(\omega_e)) \tau \left(\frac{|\mu_{ef}|^2}{\omega_{fe} - \omega_r - i \gamma_{fe}} - \frac{2 |\mu_{ge}|^2}{\omega_{eg} - \omega_r - i \gamma_{eg}} \right) / 10 \hbar^2 \quad (4)$$

where μ_{ij} are transition dipole matrix elements and γ_{ij} transverse relaxation rates between states i and j . The linear susceptibility of the material is $\chi^{(1)}(\omega_e) = N |\mu_{ge}|^2 / 3 \hbar \varepsilon_0 (\omega_{eg} - \omega_e - i \gamma_{eg})$. It is related to the absorption of the sample at wavelength λ by $\alpha = 2 \pi \text{Im} (\chi^{(1)}) / n \lambda$. The refractive index of organic materials is $n \approx 1.5$ ($n \approx 3.5$ in GaAs). An intrinsic element of comparison between nonlinear optical materials is thus:

$$\chi^{(3)} / \alpha \tau \approx 3 \varepsilon_0 n^2 \lambda^2 \Delta \sigma / 40 \pi^2 \hbar. \quad (5)$$

It represents the net optical switching efficiency per absorbed photon. It is also the switching efficiency per excited molecule and it is proportional to the average molecular absorption cross-section variation between ground and excited states $\Delta\sigma$ ($\sigma = \alpha/N$). Using equation (3) and taking $\alpha \approx 10^7 \text{ m}^{-1}$, a good figure of merit is : $\chi^{(3)}/\alpha\tau \geq 10^{-10} \text{ m}^3 \text{ V}^{-2} \text{ s}^{-1}$. It is satisfied when $\Delta\sigma \geq 2 \times 10^{-15} \text{ cm}^2$. Table II gives a comparative evaluation of materials tested at resonance. Their switching efficiencies span over 4 orders of magnitude.

Table II. — *Switching efficiencies of resonant nonlinear materials obtained from saturable absorption (sa) and photochromism (pc) experiments.*

| Materials | $\chi^{(3)}/\alpha\tau$ ($10^{-10} \text{ m}^3 \text{ V}^{-2} \text{ s}^{-1}$) | Ref. |
|--|--|------|
| Cs vapor | 1 (sa) | 11 |
| C ₆₀ | 0.03 (pc) | 12 |
| Au colloid | 0.4 | 13 |
| CdS _x Se _{1-x} glass | 0.5 (sa) | 14 |
| PTS crystal | 80 (sa) | 15 |
| 9 740 Kodak dye | 2 (sa) | 16 |
| AsGa bulk | 30 (sa) | 17 |
| AsGa MQW | 300 (sa) | 18 |
| Thermal effect | 0.1 | 10 |
| cis-trans isomery | 0.01 (pc) | 19 |
| Bacteriorhodopsin | 0.05 (pc) | 20 |
| α 6-thiophene | 1 (pc) | 21 |

The fully resonant nonlinearities which can be described by simplified three-level schemes are named photochromism in the literature [22]. Few parameters are necessary in order to characterize photochromism in terms of switching efficiency. Large nonlinearities within acceptable switching times and thicknesses are obtained in resonance with fully spin and parity allowed transitions. The efficiency to populate an excited state e depends on the quantum efficiency ϕ of conversion of the absorbed photons. Transitions are characterized by their oscillator strengths $f = 2 m_e \mu_{ij}^2 \omega_{ij} / e^2 \hbar$. They are close to unity in most organic dyes. Cross-sections of real (inhomogeneously broadened) absorptions are proportional to the inverse line-width Γ^{-1} (hwhm) of the absorption profile. The magnitude of the switching efficiency (5) can then be written as $\chi^{(3)}/\alpha\tau = A\phi f \omega_l / \Gamma_{ef}$ with $A = n c e^2 / 20 m_e \hbar \omega_e \omega_l^2$. For visible (2 eV) to infrared (1 eV) optical conversion, $A = 7.8 \times 10^{-13} \text{ m}^3 \text{ V}^{-2} \text{ s}^{-1}$. The dimensionless figure of

merit which characterizes efficient photochromic effects is thus

$$\bar{\mathcal{F}} = \phi f \omega_{\nu} / \Gamma_{ef} \gg 10^2. \quad (6)$$

The largest $\bar{\mathcal{F}}$ values are obtained with narrow excited state transitions.

Transient photochromism in conjugated oligomers.

We have performed time resolved pump-probe experiments in order to record the photoinduced (excited-state) absorption spectra of conjugated molecules [21]. The spectra of real and imaginary parts of the anisotropic phase variations photoinduced in an α -tertiophene (α -3T) solution are represented in figure 1. The optical density ($6 \delta\varphi/2.3$) induced at $\lambda_t = 603$ nm is ≈ 0.3 , it is induced with 0.4 mJ/cm² excitation at 355 nm in the maximum (λ_{\max}) of the $S_0 \rightarrow S_1$ absorption band. The same spectrum is obtained with an excitation at 396 nm on the red side of the absorption band. The transient excited state lifetime is 175 ps and we observe the singlet state $S_1 \rightarrow S_2$ transition. The new characteristic feature observed in the transient photochromism of α -3T is the narrow 40 nm (0.12 eV FWHM) width of the absorption peak induced at 603 nm as compared to the broad 65 nm (0.6 eV FWHM) linear absorption band peaking at 355 nm in solution. This effect of spectral concentration between ground and excited state transitions is the required photochromic feature in order to build an ICOC. Indeed, the broad linear absorption ensures broad band exposure sensitivity in order to record images and the narrow transient absorption band ensures efficient readout with coherent light either in absorption or in phase. In the case of α -3T, we get $\omega_{\nu} / \Gamma_{ef} \approx 30$ in figure 1 and as $\phi f \approx 1$, the photochromic OASLM figure of merit defined by equation (6) is $\bar{\mathcal{F}} = 30$.

$\alpha - nT$ thiophene oligomers, n being the number of repeat units, have their extinction coefficient ε increased by one-order of magnitude between ground and transient excited state. Except for $n = 4$, the studied oligomers exhibit spectral concentration of the excited state transition. Their photochromic figure of merit is $\bar{\mathcal{F}} \approx 20 - 50$. The readout frequency λ_t of an $\alpha - nT$ ICOC may be adjusted by choosing the oligomer length n . In all cases, the formation time of the singlet excited state is smaller than 10 ps and its recovery time is in the

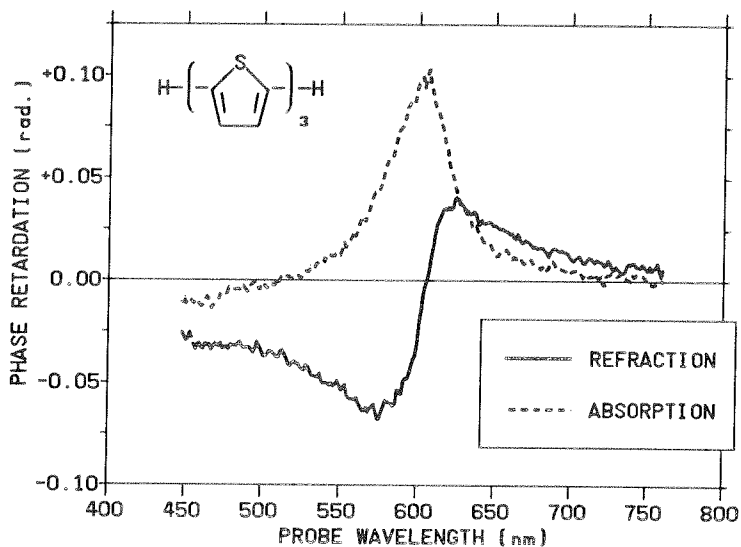


Fig. 1. — Complex phase variations induced in the thiophene oligomer α -3T.

100-200 ps range owing to intersystem crossing. Thiophene oligomers are thus potentially efficient candidates as active elements in 10 GHz ICOCs.

The photoinduced absorption of a α -6T 3 200 Å thin film is represented in figure 2 together with its linear absorption spectrum. The photoinduced absorption characteristics are independent of the pump excitation frequency. The formation time of the transient absorption is close to 50 ps and we measured a recovery time $\tau \approx 5$ ns under room conditions. This excited state is attributed to the lowest T_1 triplet state of the molecule. Spectral concentration is readily observed in figure 2 where the excited absorption peak has 0.1 eV full half-width and the ground state absorption has 1 eV full half-width. In this film, the estimated OASLM figure of merit is $\mathcal{F} \approx 60$, making it a potentially efficient candidate for 200 MHz photochromic ICOCs.

Molecular engineering of spectral concentration.

Spectral concentration in the excited state absorption results from a series of causes of which three seem essential : (1) damping of vibronic side-bands, (2) conservation of the oscillator strength, and (3) homogeneity of the molecules.

i) *Damping of the vibronic side-bands* of the ground as compared to the excited state absorption is the most characteristic feature in figure 2. Broad absorption bands are usually a peculiarity of the spectra of organic dyes as opposed to atomic and ionic absorptions. Indeed, many vibrations are closely coupled to the electronic transitions as transitions induce a change in electron densities over the bonds constituting the conjugated chain. This is the case with the $\nu_v = 1\,550\text{ cm}^{-1}$ C=C vibration producing the absorption fingers (vibronic replica) in figure 2. The fingers depend on how many sublevels are reached and how large transition moments to the sublevels are (Franck-Condon factors) [23]. After the excitation has occurred ($S_0 \rightarrow S_1$ in Fig. 3), there is a change in electron density between carbon atoms, C=C bonds are lengthened and the new equilibrium position becomes δr in figure 3. In a classical picture, carbon atoms start to oscillate around the new position with an amplitude δr . The equilibrium position is usually reached within 10^{-12} s. Narrowing of the photoinduced absorption in figure 2 comes essentially from the damping of Franck-Condon factors to the ν_v ($1\,500\text{ cm}^{-1}$) sublevels in the excited state. As pictured in figure 3, this means that the equilibrium positions of the carbon atoms are not modified in the excited state absorption $S_1 \rightarrow S_2$ (or $T_1 \rightarrow T_2$). In order for equilibrium positions of carbon atoms to remain unchanged by electronic transitions, there must be only weak localization of the long single C-C ($\approx 1.45\text{ \AA}$) and short

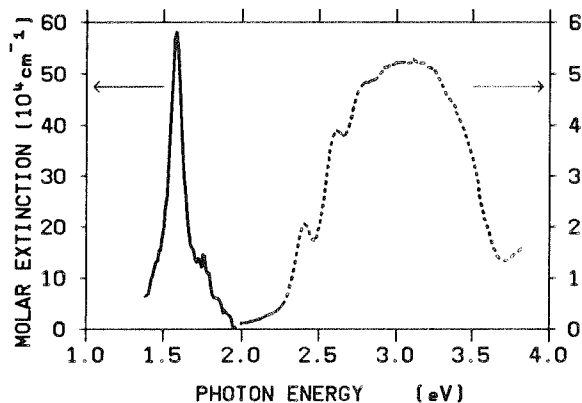


Fig. 2. — Linear (- - -) and photoinduced (—) absorption in α -6T thin films.

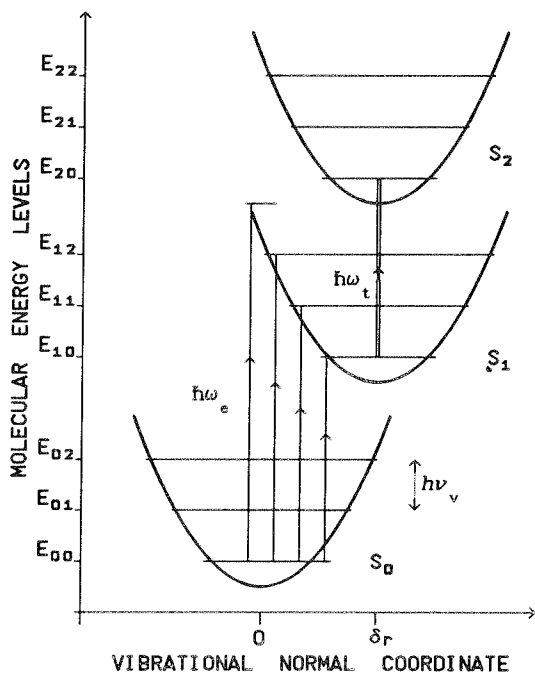


Fig. 3. — Transitions between molecular energy levels. The nuclear potential surfaces are projected along the normal coordinate of vibration, the vibronic side bands after transition to the excited state are damped.

double $C=C$ ($\approx 1.35 \text{ \AA}$) bonds along the carbon skeleton; that is that bond lengths do not alternate in the excited state as much as they do in the ground state of thiophene oligomers.

The reduction of bond alternance can be seen as a general feature of the excited state of symmetric conjugated molecules with an even number of carbon atoms in a polyene-like skeleton (Fig. 4). Indeed, their lowest energy transition is a $\pi \rightarrow \pi^*$ transition which keeps the symmetry of the molecule. The excited molecule being non-polar, as observed in α -3T [21], the excess electron pair has to be distributed symmetrically along the conjugated skeleton, thus reducing the length difference between single and double bonds. Such excited-state electron distribution is accounted for in the simplest Hückel molecular orbital theory in which the number of nodes (zeros) of the molecular orbitals increases with the energy, as do free-electron wave-functions in a quantum box [23]. Molecules in which the relative motion of carbon atoms is hindered by a ladder structure (such as condensed rings) [22] have poor performances in this respect [24]. The engineering rule for the damping of vibronic side-bands is thus to use

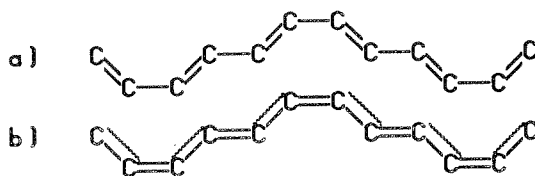


Fig. 4. — π electron distribution along the conjugated carbon skeleton of the α -3T oligomer in the ground (a) and lowest excited state (b). Dashed lines in (b) represent a symmetric repartition of the two unpaired electron which are in excess as a result of the $\pi \rightarrow \pi^*$ transition.

molecules with a conjugated polyene-like skeleton having the possibility of bond-length change upon optical excitation.

ii) *Conservation of the oscillator strength* is typical of the spectral concentration achieved in figure 2 in which the absorption coefficient α is increased by a factor of 10 between ground and excited states. The sum rule states that over the whole UV-IR spectrum, absorption verifies

$$\int \alpha(\omega) d\omega = \text{Cte} . \quad (7)$$

In order for the relevant photoinduced transition to satisfy equation (7), it is necessary to have a large quantum efficiency ϕ of transient excited state formation. By nature, singlet (S_1) states verify $\phi = 1$. Their lifetimes are in the 0.1-100 ns range. Triplet states (T_1) may also have large population efficiencies $\phi \approx 1$ from the S_1 state (intersystem crossing). Large quantum efficiencies of triplet state formation are found in aromatic molecules [25]. Their lifetimes span the 100 ns-100 ms range.

The lowest energy fully spin and parity allowed electronic transition in conjugated dyes has an oscillator strength $f \geq 1$. Long symmetric conjugated molecules such as polythiophenes have C_{2h} symmetry. The ground state S_0 wave function is usually 1A_g (even with respect to inversion). The lowest excited S_1 state is 1B_u and the second S_2 excited state has the same 1A_g symmetry as the ground state. The most coupled states are usually the closest in energy because the number of nodes of their wave functions differ only by one unit. Calculations performed in polyenes up to the octatetraene [26] show that the oscillator strength of the $S_1 \rightarrow S_2$ transition is a factor of 4 larger than that of the $S_0 \rightarrow S_1$ transition. We measured the characteristics of the lowest two-photon state of poly(3-octylthiophene) and we indeed found that the oscillator strength of the $S_1 \rightarrow S_2$ transition is $f \approx 5$ [27]. An engineering rule to achieve large excited-state oscillator strengths is to use long conjugated molecules with one-dimensional symmetry.

iii) *Homogeneity of the molecules* is a necessity in order to reach an excited state in which all absorptions are at the same frequency. This rules out the use of polymers which have not a well defined effective conjugation length. Polymers have photoinduced spectra which cover the visible spectrum as would do mixtures of oligomers. This is the case of polydiacetylene [28] though on the other hand it is a highly nonlinear material (Tab. II) [15].

Simple polyenes often undergo *cis-trans* isomerisation upon photoexcitation [22]. This can be overcome using cyclic monomers such as phenyls, thiophenes and pyrroles. They show a large ground-state conformational disorder of the inter-ring angle θ owing to free rotation around the single bond (Fig. 5) [29]. $\pi \rightarrow \pi^*$ transitions roughly correspond to a motion of the double bonds from the cyclic to the quinoid form in figure 5. This inhibits free inter-ring rotation, thus increasing the homogeneity of the excited state structure. Beside lattice and environment effects, an engineering rule for the homogeneity of the excited state transition is thus to use relatively short, up to $n \approx 10$, and regular linear oligomers made of cyclic monomers.

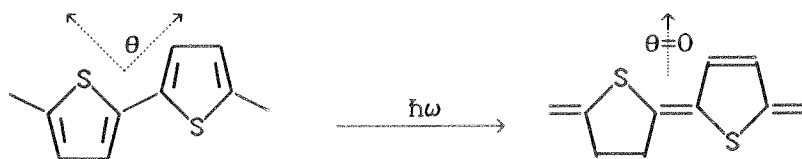


Fig. 5. — Excitation of the non-planar cyclic form to the planar quinoid form in polythiophene.

Prospects and conclusions.

More experiments are needed to determine, to control and to remove deleterious effects such as photodegradation and instability of the films. However, during our picosecond pump-probe experiments, materials exhibited good resistance. In any case, an isolated molecule can withstand more than 10^6 excitation-relaxation cycles without degradation [30]. Under 100 W/cm^2 average exposure, the lifetime of a film may thus be larger than 10 s. Moreover, as plastic films can be wound and unwound as magnetic tapes, photodegradation could be removed by cycling as in liquid organic laser dyes.

On the one hand, realization of organic OASLMs using thin films in which optical modulation is achieved on a molecular scale opens the door to devices processing large densities of parallel information (images). On the other hand, organic materials have an ultrafast response time and a relaxation time in the ns to μs range, opening the door to optical image processing at MHz to GHz frequencies. In this respect, spectral concentration permits achievement of the highest possible optical exposure sensitivities without using amplification nor etalon effects. Knowledge of the molecular engineering rules of spectral concentration will ease the tailoring of molecules with optimized switching time and exposure-readout frequencies. A future target is typically to handle diode laser beams either in amplitude or in phase, to tune the excited state lifetime in order to match the studied transients, while keeping white-light exposure sensitivities within the 1 pJ/pixel level. For instance, control of the switching time of the OASLM would permit handling of the 800 nm beam of a diode laser under day-light exposure. The required switching (or integration) time would have to be close to $1 \mu\text{s}$ with $\approx 100 \text{ W/cm}^2$ illumination on the film. It must be mentioned that owing to energy consumption and dissipation problems, GHz modulation rates would have to be limited to specific ultrafast transient analysis problems. Meanwhile, MHz rates are within the limits of low switching energy OASLM materials (Tab. I). In this respect, triplet states of organic molecules which have relaxation rates in the kHz to MHz range at room temperature are promising candidates. Thiophene oligomers exhibit spectral concentration, they have photochromic performances which make them prototypes of active elements in optimized ultrafast incoherent to coherent optical converters.

Acknowledgements.

This work was supported by the Direction des Recherches, Etudes et Techniques. We thank Doctor J. M. C. Jonathan for helpful discussions. We also thank Doctor D. Fichou for his collaboration on thiophene oligomer studies.

References

- [1] VANDERLUGT A., Optical signal processing (Wiley, New York, 1992).
- [2] BIEDERMANN K., Silver halide photographic materials, Holographic recording materials, H. M. Smit Ed. (Springer, Berlin, 1977) p. 21.
- [3] GRINBERG J., JACOBSON A., BLEHA W., MILLER L., FRAAS L., BOSWELL D. and MYER G., A new real time non coherent to coherent light image converter : the hybrid field effect liquid-crystal light valve, *Opt. Eng.* **14** (1975) 217.
- [4] JOHNSON K., Flat panel displays or bust? *Phys. World* **5** (1992) 37.
- [5] YU J. W., PSALTIS D., MARRAKCHI A., TANGUAY A. R. Jr. and JOHNSON R. V., The photorefractive incoherent to coherent optical converter, Photorefractive materials and their applications II, P. Gunter and J. P. Huignard Eds. (Springer, Berlin, 1989) p. 275.

- [6] LIVESCU G., MILLER D. A. B., HENRY J. E., GOSSARD A. C. and ENGLISH J. H., Spatial light modulator and optical dynamic memory using a 6×6 array of self-electro-optic-effect (SEED) devices, *Opt. Lett.* **13** (1988) 297.
- [7] SFEZ B. G., RAO E. V. K., NISSIM Y. I. and OUDAR J. L., Operation of nonlinear GaAs/AlGaAs multiple quantum well microresonators fabricated using alloy-mixing techniques, *Appl. Phys. Lett.* **60** (1992) 607.
- [8] KAJZAR F., MESSIER J., NUNZI J. M. and RAIMOND P., Third-order materials : processes and characterization, *Polymers for Lightwave and Integrated Optics : Technology and Applications*, L. A. Hornak Ed. (Marcel Dekker, New York, 1992) p. 595.
- [9] SMITH H. M., Basic holographic principles, *Holographic recording materials*, H. M. Smith Ed. (Springer, Berlin, 1977) p. 1.
- [10] STEGEMAN G. L., Nonlinear optical devices : current status of organics, *Organic materials for Nonlinear Optics II*, R. A. Hann and D. Bloor Eds., Special publication of the Royal Society of Chemistry (London, 1991) p. 311.
- [11] ORIA M., BLOCH D., FICHET M. and DUCLOY M., Efficient phase conjugation of a cw low-power laser diode in a short cesium (Cs) vapor cell at 852 nm, *Opt. Lett.* **14** (1989) 1082.
- [12] PALIT D. K., SAPRE A. V., MITTAL J. P. and RAO C. N. R., Photophysical properties of the fullerenes, C_{60} and C_{70} , *Chem. Phys. Lett.* **195** (1992) 1.
- [13] HACHE F., RICARD D., FLYTZANIS C. and KREIBIG U., The optical Kerr effect in small metal particles and metal colloids : the case of gold, *Appl. Phys. A* **47** (1988) 347.
- [14] ROUSSIGNOL P., RICARD D. and FLYTZANIS C., Nonlinear optical properties of commercial-semiconductor doped glasses, *Appl. Phys. A* **44** (1987) 285.
- [15] GREENE B. I., ORENSTEIN J., MILLARD R. R. and WILLIAMS L. R., Nonlinear optical response of excitons confined to one dimension, *Phys. Rev. Lett.* **58** (1987) 2750.
- [16] KOECHNER W., Solid-state laser engineering (Springer, Berlin, 1976) p. 465, $\chi^{(3)}/\alpha\tau = \epsilon_0 n^2 c\lambda/3 \pi \tau I_s$ in saturable absorbers with saturation intensity I_s and recovery time τ .
- [17] OUDAR J. L., Transient nonlinear optical effects in semiconductors, *Nonlinear optics materials and devices*, C. Flytzanis and J. L. Oudar Eds. (Springer, Berlin, 1986) p. 91.
- [18] CHEMLA D. S., Nonlinear interactions and excitonic effects in semiconductors quantum wells, *Nonlinear optics materials and devices*, C. Flytzanis and J. L. Oudar Eds. (Springer, Berlin, 1986) p. 65.
- [19] LESSARD R. A., COUTURE J. J. A. and GALARNEAU P., Application of third-order nonlinearities of dyed PVA to real time holography, *Nonlinear Optical effects in organic polymers*, J. Messier, F. Kajzar, P. Prasad and D. Ulrich, *NATO ASI Series E* **162** (Kluwer, Dordrecht, 1991) p. 343.
- [20] THOMA R., HAMPP N., BRÄUCHLE C. and OESTERHELT D., Bacteriorhodopsin films as spatial light modulators for nonlinear-optical filtering, *Opt. Lett.* **16** (1991) 651.
- [21] CHARRA F., FICHOU D., NUNZI J. M. and PFEFFER N., Picosecond photoinduced dichroism in solutions of thiophene oligomers, *Chem. Phys. Lett.* **192** (1992) 566. Cross-section σ in cm^2 and ϵ in liter/(cm.mole) verify $\sigma = 0.385 \times 10^{-20} \epsilon$.
- [22] DESSAUER R. and PARIS J. P., Photochromism, *Advances in Photochemistry*, **1** (Interscience, New York, 1963) p. 275.
- [23] SALEM L., The molecular orbital theory of conjugated systems (Benjamin, New York, 1966) p. 333.
- [24] BEESON K. W., YARDLEY J. T. and SPEISER S., All optical switching by organic nonlinearly absorbing molecules, *Nonlinear optical properties of organic materials III*, F. Khanarian Ed., *SPIE proc.* **1337** (1990) 364.
- [25] WILKINSON F., Triplet quantum yields and singlet-triplet intersystem crossing, *Organic molecular photophysics*, J. B. Birks Ed. **2** (Wiley, New York, 1975) p. 95.
- [26] HEFLIN J. R., WONG K. Y., ZAMANI-KHAMIRI O. and GARITO A. F., Nonlinear optical properties of linear chains and electron-correlation effects, *Phys. Rev. B* **38** (1988) 1573.
- [27] PFEFFER N., RAIMOND P., CHARRA F. and NUNZI J. M., Determination of the two-photon absorption spectrum of a soluble polythiophene, *Chem. Phys. Lett.* **201** (1993) 357.
- [28] CHARRA F. and NUNZI J. M., Relaxation of one- and two-photon excitations in a polydiacetylene red form : a frequency and phase resolved analysis, *Organic molecules for nonlinear optics and*

photonics, J. Messier, F. Kajzar, P. Prasad Eds., *NATO ASI Series E* **194** (Kluwer, Dordrecht, 1991), p. 359.

- [29] LOPEZ-NAVARRETE J. T., TIAN B. and ZERBI G., Chain flexibility in polyheteroatomic polymers : electronic properties, structure and vibrational spectra of oligomers as models of polypyrrole and polythiophene, *Synth. Metals* **38** (1990) 299.
- [30] RAUE R. and HARNISCH H., Dyestuff lasers and light collectors : two new fields of application for fluorescent heterocyclic compounds, *Heterocycles* **21** (1984) 167.

